HHS Public Access

Author manuscript

Cell Rep. Author manuscript; available in PMC 2016 June 29.

Published in final edited form as:

Cell Rep. 2016 June 28; 16(1): 201–212. doi:10.1016/j.celrep.2016.05.062.

Hepatic fatty acid oxidation restrains systemic catabolism during starvation

Jieun Lee[1], **Joseph Choi**[1], **Susanna Scafidi**[2], and **Michael J. Wolfgang**[1,*]

[1]Department of Biological Chemistry, Johns Hopkins University School of Medicine, Baltimore, Maryland 21205

[2]Anesthesiology and Critical Care Medicine Center for Metabolism and Obesity Research, Johns Hopkins University School of Medicine, Baltimore, Maryland 21205

Abstract

The liver is critical for maintaining systemic energy balance during starvation. To understand the role of hepatic fatty acid β-oxidation on this process, we generated mice with a liver-specific knockout of carnitine palmitoyltransferase 2 ($Cpt2^{L-/-}$), an obligate step in mitochondrial long-chain fatty acid β-oxidation. Fasting induced hepatic steatosis and serum dyslipidemia with an absence of circulating ketones while blood glucose remained normal. Systemic energy homeostasis was largely maintained in fasting $Cpt2^{L-/-}$ mice by adaptations in hepatic and systemic oxidative gene expression mediated in part by Pparα target genes including procatabolic hepatokines Fgf21, Gdf15 and Igfbp1. Feeding a ketogenic diet to $Cpt2^{L-/-}$ mice resulted in severe hepatomegaly, liver damage and death with a complete absence of adipose triglyceride stores. These data show that hepatic fatty acid oxidation is not required for survival during acute food deprivation but essential for constraining adipocyte lipolysis and regulating systemic catabolism when glucose is limiting.

Graphical Abstract

*Address correspondence to: Michael J. Wolfgang, Ph.D, Department of Biological Chemistry, Johns Hopkins University School of Medicine, 855 N. Wolfe St., 475 Rangos Building, Baltimore, MD 21205, Tel: 443-287-7680, mwolfga1@jhmi.edu.

Accession Numbers

The Gene Expression Omnibus (GEO) accession number for the mRNA expression data reported in this paper is GSE76079.

Conflict of Interest

The authors have no competing financial interests.

Author Contributions

J.L., J.C., S.S., and M.J.W. performed experiments and wrote the manuscript.

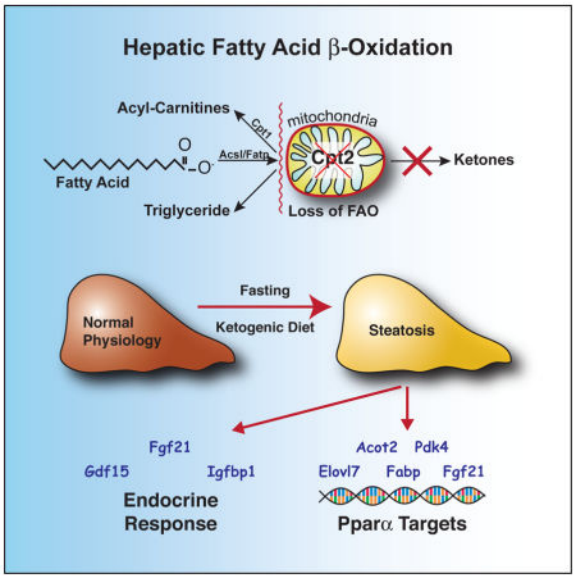

eToc

Lee et al. have generated mice that lack mitochondrial long chain fatty acid β-oxidation specifically in the liver. They report that these mice can survive a 24 hour fast but not a low carbohydrate ketogenic diet. Surprisingly, whole body energy expenditure is largely maintained due to increased peripheral catabolism.

INTRODUCTION

Starvation initiates a series of metabolic adaptations to enable continuous production and delivery of nutrients to critical organs, tissues and cells (1). This response is coordinated in large part by the liver that responds by liberating glucose to the circulation initially from glycogen stores followed by *de novo* glucose production (i.e. gluconeogenesis). Additionally, ketones are produced and provide an alternative energy source to glucose for highly oxidative tissues such as the brain (2). Fatty acid oxidation is critical for these processes as it provides the carbon substrate for ketogenesis (acetyl-CoA) and mitochondrial bioenergetics (ATP, NADH) to facilitate gluconeogenesis. Therefore, humans with disparate inborn errors in mitochondrial fatty acid oxidation exhibit life-threatening hypoketotic-hypoglycemia following a fast (3). Systemically, the liver produces most of the circulating ketones due to its high capacity for β-oxidation and lack of the CoA transferase (Oxct1) in hepatocytes that is required to utilize ketones (4). Also, the liver is thought to dominate fasting gluconeogenesis with minor contributions from the kidney and gut. Interestingly, mice with a hepatocyte-specific loss of glucose-6-phosphatase, the obligate terminal enzyme in cellular glucose liberation, do not exhibit reduced blood glucose following fasting or starvation, although ketone production is accelerated (5). Therefore, extra-hepatic gluconeogenic tissues can fully compensate for a loss of hepatic production.

Mitochondrial long chain fatty acid β-oxidation is governed by the regulated translocation of activated fatty acids (acyl-CoAs) from the cytoplasm to the mitochondrial matrix mediated

by successive carnitine acyltransferases (6). Carnitine Palmitoyltransfersase 1 (Cpt1) isoenzymes mediate acyl transfer from long chain acyl-CoAs to carnitine on the outer mitochondrial membrane, generating acylcarnitines that can traverse through the Carnitine-acylcarnitine translocase within the inner mitochondrial membrane. Within the mitochondrial matrix, Cpt2 transfers the acyl group from the acylcarnitine back onto CoA, enabling β-oxidation. Human inborn errors in Cpt2 result in increasing severity of metabolic disease (OMIM #s, 255110 adult onset, 600649 infantile, and 600650 infantile lethal) (7, 8). The complete loss of *Cpt1a* or *Cpt1b* is embryonic lethal in mice, and the loss of *Acadl* or *Acadm* results in increased neonatal death (9–11). The loss of other mitochondrial components of β-oxidation result in multisystemic defects as well as cell-specific compensatory mechanisms (12–15).

To understand the contribution of hepatic fatty acid oxidation during fasting and starvation, we generated mice with a liver-specific knockout of Carnitine Palmitoyltransferase 2 ($Cpt2^{L-/-}$), an obligate enzyme in mitochondrial long chain fatty acid β-oxidation encoded by a single gene. To our great surprise, $Cpt2^{L-/-}$ mice not only survived the perinatal period but also did not exhibit alterations in blood glucose following a 24hr fast although ketones were absent. Fasting resulted in serum dyslipidemia, hepatic steatosis and alterations in hepatic and systemic oxidative gene expression. Although $Cpt2^{L-/-}$ mice were able to adapt to survive a 24hr fast, feeding them a ketogenic diet resulted in hepatomegaly and death after only 6 days with a complete absence of adipose triglyceride stores. These data show that hepatic fatty acid oxidation is not required for survival during acute food deprivation, but is essential for constraining adipocyte lipolysis and regulating systemic catabolism when glucose is limiting.

RESULTS

Generation of mice with a liver-specific deficiency in fatty acid β-oxidation

Previously, we generated a mouse model with a conditional loss-of-function allele for *Cpt2*, an obligate step in mitochondrial long chain fatty acid β-oxidation (16, 17). To produce mice with a loss of Cpt2 specifically in hepatocytes, we bred $Cpt2^{lox/lox}$ mice to liver-specific albumin-Cre transgenic mice (18). The resulting liver-specific Cpt2 knockout (KO) mice ($Cpt2^{L-/-}$) showed a loss of Cpt2 protein in the liver (Figure 1A) and decreased mRNA levels of *Cpt2* specifically in the liver (Figure 1B). As expected, oleate oxidation was significantly suppressed in the liver of $Cpt2^{L-/-}$ mice to a similar degree as incubation with 100μM of the CPT inhibitor, etomoxir (19). There was no change in the oxidation of the very long chain fatty acid, lignoceric acid, which is preferentially oxidized in peroxisomes (Figure 1C). Although males had a small suppression of body weight after weaning, females did not show suppressed body weight and all mice exhibited normal body weight by 6 weeks of age (Figure 1D). These data show that the loss of hepatic mitochondrial long chain fatty acid β-oxidation is not required for survival to adulthood. This is surprising given the requirement for fatty acid β-oxidation during the perinatal period (15, 20, 21).

Fasting results in hypoketotic dyslipidemia in Cpt2$^{L-/-}$ mice

To determine the requirements for hepatic fatty acid oxidation upon food deprivation, we fasted Cpt2$^{lox/lox}$ and Cpt2$^{L-/-}$ mice for 24 hours at 9 weeks of age. As expected, there was a significant decrease in serum β-hydroxybutyrate (βHB) in Cpt2$^{L-/-}$ mice even in the fed state. Control Cpt2$^{lox/lox}$ mice dramatically increased serum βHB upon a 24hr fast as expected while Cpt2$^{L-/-}$ mice did not exhibit appreciable serum βHB consistent with the a loss of hepatic fatty acid oxidation (Figure 2A). Additionally, fasting induced serum dyslipidemia with increased NEFA and cholesterol in Cpt2$^{L-/-}$ mice (Figure 2A). Cpt2$^{L-/-}$ mice did not become hypoglycemic following the 24hr fast nor was insulin different between geneotypes (Figure 2A). Because the liver plays an integral role in fatty acid metabolism in the body, we determined whole body bioenergetics in Cpt2$^{L-/-}$ mice. Interestingly, there was no change in energy expenditure between Cpt2$^{lox/lox}$ and Cpt2$^{L-/-}$ mice in fed, fasted, or refed states (Figure 2B). Although Cpt2$^{L-/-}$ mice exhibit clear metabolic deficiencies, in the context of whole animal energy homeostasis, Cpt2$^{lox/lox}$ and Cpt2$^{L-/-}$ mice were able to maintain equivalent energy expenditure and respiratory exchange ratio even during fasting (Figure 2B). Food intake, body composition, and ambulatory activity were not different between male or female Cpt2$^{lox/lox}$ and Cpt2$^{L-/-}$ mice (Figures 2C and S1A–D). Examination of tissue weights in Cpt2$^{lox/lox}$ and Cpt2$^{L-/-}$ mice showed that fasting resulted in a greater suppression in gonadal white adipose tissue (gWAT) in Cpt2$^{L-/-}$ mice while there was a concomitant increase in liver weight (Figure 2D). Consistent with the wet weight data, Cpt2$^{L-/-}$ livers were enlarged and lipid laden following a 24-hour fast (Figure 2E). Liver triglyceride levels were unchanged in the fed state but were significantly increased in Cpt2$^{L-/-}$ mice compared to control Cpt2$^{lox/lox}$ mice upon fasting (Figure 2F). There were not signs of liver damage by serum ALT activity (Figure 2G), altered corticosterone levels (Figure S1E), or significant markers of ER stress (Figure S1F) following a 24 hour fast. However, Cpt2$^{L-/-}$ livers did show significant lipid peroxidation following fasting (Figure 2H). These data show that mice with a loss of hepatic fatty acid β-oxidation can adapt to maintain systemic energy homeostasis during a fast but not without adverse consequences to the liver and adipose tissue stores.

Fasting increases oxidative and suppresses lipogenic programing in livers of Cpt2$^{L-/-}$ mice

Given the robust physiological and cellular adaptations in Cpt2$^{L-/-}$ mice, we determined hepatic gene expression of select fatty acid metabolic genes in fed and fasted Cpt2$^{lox/lox}$ and Cpt2$^{L-/-}$ mice. First we determined the expression of fatty acid oxidation genes. In the fed state, there were increases in *Acsl1, Acot1* and *Acot2* mRNA in the livers of Cpt2$^{L-/-}$ mice (Figure 3A). Acot1 and Acot2 were also increased at the protein level in the livers of fed Cpt2$^{L-/-}$ mice (Figure 3B). Following a 24-hour fast, the increases in *Acot1* and *Acot2* in the livers of fed Cpt2$^{L-/-}$ mice were greatly exacerbated as well as increases in the fatty acid oxidative genes, *Acox1*, *Acadl* and *Hadha* (Figure 3A). These changes were largely mirrored at the protein level by western blotting (Figure 3B). Many of the fatty acid biosynthetic genes were suppressed following a 24hr fast in livers of Cpt2$^{L-/-}$ mice compared to Cpt2$^{lox/lox}$ mice (Figures 3B, S2A). Gluconeogenic gene expression was not altered in Cpt2$^{L-/-}$ mice with the exception of *Pck2* whose contribution to gluconeogenesis is not well defined (Figure S3A). These data show a robust up-regulation of fatty acid catabolic genes

and suppression of fatty acid anabolic genes in the livers of Cpt2$^{L-/-}$ mice that were exacerbated by fasting. This suggests that the fatty acid oxidation deficient livers were attempting to compensate for the lack of fatty acid oxidation in the face of a large lipid burden.

Fasting induces Pparα target genes and procatabolic hepatokines Fgf21, Gdf15, and Igfbp1 in Cpt2$^{L-/-}$ mice

Due to the robust transcriptional response in Cpt2$^{L-/-}$ mice, we decided to probe further into the transcriptional alterations in the livers of Cpt2$^{L-/-}$ mice. Therefore, we fasted Cpt2$^{lox/lox}$ and Cpt2$^{L-/-}$ mice for 24hrs for genome wide gene expression profiling on liver mRNA via DNA microarrays (Table 1). Microarray analysis revealed a dramatic transcriptional dysregulation in the livers of Cpt2$^{L-/-}$ mice upon fasting. In order to validate the microarray results in a larger cohort of mice, we analyzed a subset of genes identified in the microarray analysis by qRT-PCR in both fed and fasted Cpt2$^{lox/lox}$ and Cpt2$^{L-/-}$ mice (Table 1). Consistent with the robust transcriptional and protein induction of Acot1 and Acot2, other type I ACOTs, canonical Pparα target genes, were also identified in the microarray. Other canonical Pparα target genes were also dramatically up-regulated such as *Pdk4* (~100 fold), *Ehhadh* (~50 fold), *Cd36*, (~10 fold), and *Fabp3* (~160 fold) (Table 1). These data suggest that exogenous fatty acid derived Pparα ligands build up in the face of increased lipid delivery to the liver and are greatly potentiated in the absence of mitochondrial fatty acid oxidation.

We were surprised that although Cpt2$^{L-/-}$ mice had clear metabolic deficiencies, they were able to maintain systemic energy homeostasis even following a 24hr fast. Therefore, we were interested in determining how the Cpt2$^{L-/-}$ liver might be communicating these deficits with other tissues. Of interest was one of the most highly up-regulated genes in the livers of Cpt2$^{L-/-}$ mice (~50 fold), the secreted hepatokine *Fgf21* (Table 1, Figure 3C). *Fgf21* is also a canonical Pparα target gene (22, 23). Consistent with the transcriptional increase in *Fgf21*, serum Fgf21 was increased (~11.5 fold) in fasted Cpt2$^{L-/-}$ mice compared with Cpt2$^{lox/lox}$ littermate controls (Figures 3D). Additionally, *Gdf15* and *Igfbp1* mRNA were increased in fasted Cpt2$^{L-/-}$ liver and these were also increased to a similar degree in Cpt2$^{L-/-}$ serum (Figures 3C,D). These secreted proteins have all been shown to increase systemic catabolism (22–26). These data suggest that the loss of hepatic fatty acid oxidation is mitigated in part by increasing systemic procatabolic hepatokines.

Fasting induces systemic catabolic gene expression in Cpt2$^{L-/-}$ mice

Some metabolic processes that occur largely in the liver, such as gluconeogenesis, can be supplanted in part by the kidney. Therefore, we postulated that the kidney could be a major site of systemic compensation of energy homeostasis. First, we assessed the regulation of oxidative gene expression in the kidneys of fed and 24hr fasted Cpt2$^{lox/lox}$ and Cpt2$^{L-/-}$ mice. Fasting initiated a robust increase in the expression of genes involved in fatty acid oxidation in the kidneys of Cpt2$^{L-/-}$ mice similar to the elevation in liver (Figure 4A). A subset of these genes were also validated at the protein level (Figure 4B). Similar to the liver, gluconeogenic gene expression was not altered in Cpt2$^{L-/-}$ mice with the exception of *Pck2* (Figure S3B). Upon dissection, the kidneys of 24hr fasted Cpt2$^{L-/-}$ mice were visibly lipid

laden (Figure 4C). Although the wet weight of the kidneys of $Cpt2^{lox/lox}$ and $Cpt2^{L-/-}$ mice were similar, the kidneys of $Cpt2^{L-/-}$ mice exhibited a ~2fold increase in total triglycerides consistent with increased uptake of fatty acids (Figures 4D,E). These data support the kidney as a major site of compensation in fasted $Cpt2^{L-/-}$ mice.

Fgf21 has been shown to regulate ketogenic and oxidative genes in the liver in an autocrine manner. Fgf21 has also been postulated to affect adipocyte energy balance in an endocrine manner (27). Since fasting induces a robust increase in circulating Fgf21 in $Cpt2^{L-/-}$ mice, we examined some of the putative endocrine effects of Fgf21 treatment in a more physiological model. Interscapular BAT (iBAT) of $Cpt2^{L-/-}$ mice did not exhibit transcriptional increases in thermogenic genes (Figure 4F), but fasting elicited increases in *Ucp1*, *Cidea* and *Fgf21* in inguinal WAT (iWAT) of $Cpt2^{L-/-}$ mice (Figure 4G) consistent with fasting induced Fgf21 target gene expression in this tissue (28). Adipose-derived Adiponectin has also been shown to be a pharmacologic target of Fgf21 (29, 30). However, we did not observe an increase in adiponectin mRNA in gonadal WAT (gWAT) nor did we observe changes in serum Adiponectin between fed or fasting $Cpt2^{lox/lox}$ and $Cpt2^{L-/-}$ mice (Figure 4H). Due to the robust contribution of skeletal muscle and heart to whole body fatty acid oxidation, we examined fatty acid oxidative gene expression in these tissues. Although the transcriptional response was not as robust as the kidney in these tissues, fasting induced a significant increase in *Acot1* and *Acot2* in $Cpt2^{L-/-}$ gastrocnemius muscle (Figure 4I) and induced a significant increase in *Acot1* in the $Cpt2^{L-/-}$ heart (Figure S3C). Interestingly, along with liver and iWAT, skeletal muscle of $Cpt2^{L-/-}$ mice also exhibited a significant fasting induced increase in *Fgf21* expression (Figure 4J). Together, these data suggest that loss of hepatic fatty acid oxidation may be mitigated in part by the induction of procatabolic hepatokines such as Fgf21 via both cell autonomous and non-cell autonomous mechanisms.

A ketogenic diet depletes adipose triglyceride stores and is lethal to $Cpt2^{L-/-}$ mice

Given the putative requirements for hepatic fatty acid oxidation, we were surprised that $Cpt2^{L-/-}$ mice could survive a 24hr fast. To determine how $Cpt2^{L-/-}$ mice would tolerate a long-term carbohydrate-limited diet, we placed 9-week old $Cpt2^{lox/lox}$ and $Cpt2^{L-/-}$ mice on a low carbohydrate ketogenic diet. After 6 days on the ketogenic diet, several $Cpt2^{L-/-}$ mice died and the remaining $Cpt2^{L-/-}$ mice exhibited a dramatic weight loss (Figure 5A). $Cpt2^{L-/-}$ mice exhibited hepatomegaly (Figure 5B) and significant liver damage as measured by serum ALT activity (Figure 5C). These physiologic indicators were accompanied by severe kyphosis and lethargy, suggesting a neurologic involvement. Additionally, $Cpt2^{L-/-}$ mice became hypoglycemic and hypoketotic with corresponding serum dyslipidemia (Figure 5D). Incredibly, upon dissection, $Cpt2^{L-/-}$ mice completely lacked observable white adipose tissue following 6 days on a ketogenic diet, consistent with the loss of body weight (Figure 5E). These data suggest that from a physiological standpoint, $Cpt2^{L-/-}$ mice could not differentiate starvation from a high calorie-low carbohydrate diet.

Fasting and a ketogenic diet share many metabolic features. Therefore we assessed the gene expression signature of $Cpt2^{lox/lox}$ and $Cpt2^{L-/-}$ mice fed a ketogenic diet for 6 days. Consistent with the microarray data from 24hr fasting liver, the livers from $Cpt2^{L-/-}$ mice

exhibited a dramatic increase in Pparα-target gene expression compared to control $Cpt2^{lox/lox}$ mice (~170 fold increase in *Pdk4*, >50 fold increase in *Elovl7*) (Table 1). Also, oxidative gene expression in the livers of $Cpt2^{L-/-}$ mice was increased in ketogenic diet fed mice (Figure 5F). Gluconeogeneic gene expression, serum insulin and oxidative gene expression in the kidney, gastrocnemius muscle and heart were also consistent with the fasting data (Figure S4). Finally, we measured the gene expression (Table 1) and serum concentrations of the secreted hepatokines Fgf21, Gdf15, and Igfbp1 (Figure 5G). Even though the ketogenic diet elicited a strong induction of these heptokines in control $Cpt2^{lox/lox}$ mice, $Cpt2^{L-/-}$ mice further exacerbated this increase in serum hepatokines. These data show that the ketogenic diet elicits a similar yet further exacerbated physiologic program in $Cpt2^{L-/-}$ mice compared to fasting.

To better determine the kinetics of the ketogenic-induced weight loss and hypoglycemia in mice deficient in hepatic fatty acid β-oxidation, we again placed $Cpt2^{lox/lox}$ and $Cpt2^{L-/-}$ mice on a ketogenic diet and measured their body weights and blood glucose daily over 4 days. $Cpt2^{lox/lox}$ and $Cpt2^{L-/-}$ mice had no significant differences in fed blood glucose (Figure 6A) or body weight (Figure 6B) over these 4 days although by day 4, $Cpt2^{L-/-}$ mice had accelerated body weight loss. This indicates that a lack of systemic gluconeogenesis was not the primary cause of lethality in $Cpt2^{L-/-}$ mice.

To determine the systemic metabolic effects of a loss of hepatic Cpt2, we measured blood and tissue acylcarnitines in $Cpt2^{lox/lox}$ and $Cpt2^{L-/-}$ mice before and over the 4-day ketogenic diet challenge. As the liver is a major site of carnitine biosynthesis, there were no changes in free carnitine in the liver; however, there was a significant suppression in free carnitine in the blood of $Cpt2^{L-/-}$ mice, indicating a systemic deficiency (Figure 6C). Total acylcarnitines and short chain acylcarnitines were significantly suppressed in both chow and ketogenic diet fed blood of $Cpt2^{L-/-}$ mice (Figure 6D, Table S1). However, the substrates specific for Cpt2, long chain acylcarnitines, showed a progressive increase in blood over time, indicating increased hepatic excursion of long chain acylcarnitines in $Cpt2^{L-/-}$ mice (Figure 6E, Table S1). Finally, we measured liver acylcarnitines in chow fed and 4-day ketogenic diet fed mice. Consistent with a block in fatty acid β-oxidation, $Cpt2^{L-/-}$ mice exhibited a suppression in liver acetylcarnitine that was exacerbated by the ketogenic diet (Figure 6F), and an increase in long chain acylcarnitines even in chow fed mice (Figure 6G, Table S2). These data show that a loss of hepatic fatty acid β-oxidation results in an accelerated depletion of adipose lipid stores and increased peripheral catabolism following fasting or a ketogenic diet that is ultimately unsustainable.

DISCUSSION

The importance of fatty acid β-oxidation is made evident by multiple inborn errors in this pathway that cause serious human disease (8, 31, 32). For example, hypomorphic mutations in CPT2 result in metabolic disease of increasing severity. The most severe form presents as hypothermia, cardiomegaly, hepatomegaly and hypoglycemia in the first days of life from the important roles of fatty acid β-oxidation in adipocytes, heart and liver. Additionally, hypomorphic mutations in CPT1a result in hypoketotic-hypoglycemia (3) and a loss of CPT1a or CPT1b in mice is early embryonic lethal (9, 11). Given that the liver is critical for

the adaptation to fasting and fatty acid β-oxidation is central to this response, we asked what the requirements of hepatic fatty acid β-oxidation are *in vivo*. Surprisingly, we found that mice with a hepatocyte-specific deletion of mitochondrial long chain fatty acid β-oxidation not only survived the perinatal period but also survived a 24hr fast with normal blood glucose but a lack of ketone bodies. Perhaps not surprisingly, survival during food deprivation has been so evolutionarily important that multiple compensatory systems are in place for such a critical adaptation.

While blood glucose is maintained within a tight range, ketones can change dramatically from μM to mM concentrations (1). Our data suggests that the liver produces almost all of the circulating ketones. The total loss of ketone utilization via KO of *Oxct1* results in perinatal lethality in mice (4). Therefore we speculate that local ketone production (e.g. within the CNS) or a small amount of fatty acid independent ketogenesis may enable the survival of $Cpt2^{L-/-}$ mice during the perinatal period, a time of robust ketolysis (33, 34). Several effects of βHB indirectly associated with its metabolic role have been suggested (35). βHB is an endogenous ligand for at least two $G_{i/o}$-coupled GPCRs, HCAR2 and FFAR3, that suppress adipose lipolysis and sympathetic activity respectively (36, 37). Given the dramatic peripheral catabolism in ketogenic diet fed $Cpt2^{L-/-}$ mice that have suppressed circulating βHB, these nonmetabolic roles of ketones likely play a significant role in regulating systemic physiology during food deprivation. The inability to affect these two receptors would lead to enhanced fasting lipolysis consistent with $Cpt2^{L-/-}$ mice. Therefore, βHB is likely critical for restraining lipolysis, particularly under conditions where insulin is low.

Pparα has been postulated to be activated by fatty acid derived ligands. Some ligands are thought to be derived from *de novo* fatty acid synthesis (38–40), however that seems to be an unlikely driver of fasting gene expression in $Cpt2^{L-/-}$ mice. Alternatively, triglyceride hydrolysis has been shown to be critical for Pparα directed transcription. The loss of Atgl, the rate setting step in triglyceride hydrolysis, results in a loss of Pparα transcription presumably from the loss of an endogenous Pparα ligand produced upon hydrolysis (41–44). It will be interesting to determine if lipids derived from lipid droplet triglyceride hydrolysis are required for the increased Pparα mediated transcription in $Cpt2^{L-/-}$ mice or alternatively, if exogenous lipid uptake can directly activate Pparα target genes independent of lipid droplets.

One robust transcriptional target of Pparα is the hepatokine Fgf21 (22, 23). Although it is expressed in several tissues, most of the circulating Fgf21 is derived from hepatocytes (45). Fgf21 is induced by fasting and ketogenic feeding in rodents and acts largely to increase energy expenditure via an autocrine and endocrine manner (27). Fgf21 is emerging as a potential therapeutic for obesity and insulin resistance by increasing glucose uptake in adipocytes and increasing energy expenditure. The robust increase in circulating Fgf21 in $Cpt2^{L-/-}$ mice suggests that it provides some of the signal required to increase systemic catabolism to maintain energy homeostasis although Gdf15 and Igfbp1 likely also contribute. Consistent with $Cpt2^{L-/-}$ mice, humans with mitochondrial disease exhibit increased circulating FGF21 (46). The loss of the anti-catabolic βHB and the gain of procatabolic hepatokines such as Fgf21, Gdf15 and Igfbp1, likely all contribute to the

exaggerated lipolysis seen in $Cpt2^{L-/-}$ mice upon fasting or ketogenic feeding, and mitigate hepatic energy expenditure defects in mice without the capacity for long chain mitochondrial fatty acid β-oxidation.

It is clear that the liver plays an important role in regulating systemic metabolism, and that hepatic fatty acid β-oxidation represents an important component, particularly when carbohydrate intake is limiting. However, our data shows that there is an incredible systemic adaptation mediated by the liver to regulate extra-hepatic metabolism to ensure survival. These data highlight the need to better understand the tissue-specific contributions of macronutrient metabolism to gain insight into the regulation of integrative metabolic physiology.

EXPERIMENTAL PROCEDURES

Animals

To generate a liver-specific loss-of-function of *Cpt2*, we bred $Cpt2^{lox/lox}$ mice (16) to albumin-Cre transgenic mice (18). Mice were housed in ventilated racks with a 14 hr light/10 hr dark cycle and fed a standard chow diet (Harlan Laboratories). All mice were euthanized at the same time of day (3p.m.). Fed mice were food deprived from 1 p.m.-3 p.m. to ensure consistent feeding patterns. For fasting studies, mice were deprived of food for 24 hours from 3p.m.-3 p.m. For the ketogenic diet studies, mice were placed on a ketogenic diet at 9 weeks of age (47). Serum was collected for all mice to measure free glycerol and TAG (Sigma), β-hydroxybutyrate (StanBio), total cholesterol, NEFA (Wako), and ALT (Sigma). Fgf21, Gdf15, Igfbp1, Corticosterone, Adiponectin (R&D systems) and insulin (Millipore) were measured by ELISA. Body fat and lean mass of 9-week old mice was measured via magnetic resonance imaging analysis (QNMR EchoMRI100; Echo Medical Systems, LLC). Indirect calorimetery and metabolic cage studies were normalized to total lean mass as described (48). All procedures were performed in accordance with the NIH's *Guide for the Care and Use of Laboratory Animals* and under the approval of the Johns Hopkins Medical School Animal Care and Use Committee.

Metabolic measurements

Blood levels of acylcarnitines were quantified from dried blood spots (DBS) with modifications (49, 50). Punched 1/8″ DBS samples were submerged in 100 μl of methanol solution containing internal standards for acyl carnitines (NSK B, Cambridge Isotopes). Samples were incubated at 4°C for 20min, dried under nitrogen and then 60 μl 3N HCl in n-butanol was added. The samples were incubated for 15 min at 65 °C then dried under LN_2, and butylated acyl carnitines were reconstituted in 100 μl of mobile phase acetonitrile/water/formic acid (H_2O:CH_3CN:HCOOH; 80:19.9:0.1 v/v%). Samples were vortexed, transferred to a centrifuge filter, spun and transferred to an injection vial. Tissue acyl carnitines were isolated from freeze-clamped tissue and homogenized in a methanol solution containing internal standards as above, sonicated for 10min at room temperature and centrifuged for 4min at 13,000rpm at 4°C. Following centrifugation, the liquid phase was collected and evaporated to dryness under LN_2 and processed as above. Acyl carnitines were analyzed on an API 3200 (AB SCIEX, Foster City, CA) operated in positive ion mode employing

precursor ion scan for m/z 85, which is generated as a characteristic product ion of butyl ester of acyl carnitine species. Quantitation of acyl carnitines was achieved by Chemoview (AB SCIEX) application. All blood samples are reported as nmol/ml; tissue samples as pmol/mg. Liver fatty acid oxidation, TAG measurement and liver peroxidation was done as previously described (47, 48).

Real Time qPCR

RNA was isolated from all tissues using the RNeasy Mini Kit (QIAGEN). Using the High Capacity cDNA Reverse Transcription Kit (Applied Biosystems), we reverse transcribed 1–2 ug of total RNA. The cDNA was diluted to 2ng/uL and amplified by primers in a 20 uL reaction using SsoAdvanced SYBR Green Supermix (Bio-Rad). The analysis was done using a CFX Connect Real-Time System (Bio-Rad). We calculated mRNA using a 2^deltaCT relative to the average of the housekeeping genes *cyclophilin A*, *rpl22* and *18s* expression. ER stress was measured as described elsewhere (51). All primers and gene information were previously reported (16).

Western Blot

Liver and kidney homogenates were prepared using 1× RIPA buffer with protease inhibitors. The protein concentration was measured using the Pierce BCA Protein Assay kit (Thermo Scientific). We used 30 ug of protein on an SDS-PAGE and then transferred it to either a nitrocellulose (Protran BA 83, Whatman) or a polyvinylidene difluoride (PVDF) membrane. We then blocked with 3% BSA-TBST (tris buffer saline with tween 20). The membranes were then probed with antibodies Cpt2 (Pierce), Pgc1α (Abcam), Acsl1 (Cell Signaling), Acot1 (Cell Signaling), Acot2 (Cell Signaling), Cpt1α (Abcam), Acadm (GeneTex), Acsf3 (Pierce), Total Acc (Cell Signaling), Acly (Cell Signaling), Hadha (Genetex), Aco2 (Cell Signaling), Fasn (BD Biosciences), and Hsc70 (Santa Cruz Biotechnology). Hsc70 used the appropriate Cy3 fluorescent secondary antibodies, and the other primary antibodies used the corresponding secondary antibodies conjugated to horseradish peroxidase. Images were collected using an Alpha Innotech FluorChemQ and presented with minimal image processing.

Statistical Analysis

Data were analyzed with the assistance of Prism. Significance was determined using an unpaired two-tailed Student’s t-test for single variable experiments and two-way ANOVA with Bonferroni post hoc correction for multiple variable experiments.

Supplementary Material

Refer to Web version on PubMed Central for supplementary material.

Acknowledgments

The authors would like to thank Susan Aja for assistance with the metabolic cage studies. This work was supported in part by a pilot and feasibility award from the Mid-Atlantic Nutrition Obesity Research Center P30DK072488, American Diabetes Association grant #1-16-IBS-313 to M.J.W. and National Institutes of Health grants R01NS072241 to M.J.W. and K08NS069815 to S.S. J.L. was supported in part by T32GM007445.

References

1. Cahill GF Jr. Fuel metabolism in starvation. Annu Rev Nutr. 2006; 26:1–22. [PubMed: 16848698]
2. Owen OE, Morgan AP, Kemp HG, Sullivan JM, Herrera MG, Cahill GF Jr. Brain metabolism during fasting. J Clin Invest. 1967; 46(10):1589–95. [PubMed: 6061736]
3. LIJ, Mandel H, Oostheim W, Ruiter JP, Gutman A, Wanders RJ. Molecular basis of hepatic carnitine palmitoyltransferase I deficiency. J Clin Invest. 1998; 102(3):527–31. [PubMed: 9691089]
4. Cotter DG, d'Avignon DA, Wentz AE, Weber ML, Crawford PA. Obligate role for ketone body oxidation in neonatal metabolic homeostasis. The Journal of biological chemistry. 2011; 286(9): 6902–10. [PubMed: 21209089]
5. Mutel E, Gautier-Stein A, Abdul-Wahed A, Amigo-Correig M, Zitoun C, Stefanutti A, Houberdon I, Tourette JA, Mithieux G, Rajas F. Control of blood glucose in the absence of hepatic glucose production during prolonged fasting in mice: induction of renal and intestinal gluconeogenesis by glucagon. Diabetes. 2011; 60(12):3121–31. [PubMed: 22013018]
6. McGarry JD, Brown NF. The mitochondrial carnitine palmitoyltransferase system. From concept to molecular analysis. Eur J Biochem. 1997; 244(1):1–14. [PubMed: 9063439]
7. Isackson PJ, Bennett MJ, Lichter-Konecki U, Willis M, Nyhan WL, Sutton VR, Tein I, Vladutiu GD. CPT2 gene mutations resulting in lethal neonatal or severe infantile carnitine palmitoyltransferase II deficiency. Mol Genet Metab. 2008; 94(4):422–7. [PubMed: 18550408]
8. Longo N, Amat di San Filippo C, Pasquali M. Disorders of carnitine transport and the carnitine cycle. Am J Med Genet C Semin Med Genet. 2006; 142C(2):77–85. [PubMed: 16602102]
9. Nyman LR, Cox KB, Hoppel CL, Kerner J, Barnoski BL, Hamm DA, Tian L, Schoeb TR, Wood PA. Homozygous carnitine palmitoyltransferase 1a (liver isoform) deficiency is lethal in the mouse. Mol Genet Metab. 2005; 86(1–2):179–87. [PubMed: 16169268]
10. Kurtz DM, Rinaldo P, Rhead WJ, Tian L, Millington DS, Vockley J, Hamm DA, Brix AE, Lindsey JR, Pinkert CA, et al. Targeted disruption of mouse long-chain acyl-CoA dehydrogenase gene reveals crucial roles for fatty acid oxidation. Proceedings of the National Academy of Sciences of the United States of America. 1998; 95(26):15592–7. [PubMed: 9861014]
11. Ji S, You Y, Kerner J, Hoppel CL, Schoeb TR, Chick WS, Hamm DA, Sharer JD, Wood PA. Homozygous carnitine palmitoyltransferase 1b (muscle isoform) deficiency is lethal in the mouse. Molecular genetics and metabolism. 2008; 93(3):314–22. [PubMed: 18023382]
12. Spiekerkoetter U, Wood PA. Mitochondrial fatty acid oxidation disorders: pathophysiological studies in mouse models. Journal of inherited metabolic disease. 2010; 33(5):539–46. [PubMed: 20532823]
13. Zhang D, Christianson J, Liu ZX, Tian L, Choi CS, Neschen S, Dong J, Wood PA, Shulman GI. Resistance to high-fat diet-induced obesity and insulin resistance in mice with very long-chain acyl-CoA dehydrogenase deficiency. Cell Metab. 2010; 11(5):402–11. [PubMed: 20444420]
14. Zhang D, Liu ZX, Choi CS, Tian L, Kibbey R, Dong J, Cline GW, Wood PA, Shulman GI. Mitochondrial dysfunction due to long-chain Acyl-CoA dehydrogenase deficiency causes hepatic steatosis and hepatic insulin resistance. Proceedings of the National Academy of Sciences of the United States of America. 2007; 104(43):17075–80. [PubMed: 17940018]
15. Tolwani RJ, Hamm DA, Tian L, Sharer JD, Vockley J, Rinaldo P, Matern D, Schoeb TR, Wood PA. Medium-chain acyl-CoA dehydrogenase deficiency in gene-targeted mice. PLoS genetics. 2005; 1(2):e23. [PubMed: 16121256]
16. Lee J, Ellis JM, Wolfgang MJ. Adipose fatty acid oxidation is required for thermogenesis and potentiates oxidative stress-induced inflammation. Cell Rep. 2015; 10(2):266–79. [PubMed: 25578732]
17. Lee J, Choi J, Aja S, Scafidi S, Wolfgang MJ. Loss of Adipose Fatty Acid Oxidation Does Not Potentiate Obesity at Thermoneutrality. Cell Rep. 2016; 14(6):1308–16. [PubMed: 26854223]
18. Postic C, Shiota M, Niswender KD, Jetton TL, Chen Y, Moates JM, Shelton KD, Lindner J, Cherrington AD, Magnuson MA. Dual roles for glucokinase in glucose homeostasis as determined by liver and pancreatic beta cell-specific gene knock-outs using Cre recombinase. The Journal of biological chemistry. 1999; 274(1):305–15. [PubMed: 9867845]

19. Nomura M, Liu J, Rovira II, Gonzalez-Hurtado E, Lee J, Wolfgang MJ, Finkel T. Fatty acid oxidation in macrophage polarization. Nat Immunol. 2016; 17(3):216–7. [PubMed: 26882249]
20. Boles RG, Buck EA, Blitzer MG, Platt MS, Cowan TM, Martin SK, Yoon H, Madsen JA, Reyes-Mugica M, Rinaldo P. Retrospective biochemical screening of fatty acid oxidation disorders in postmortem livers of 418 cases of sudden death in the first year of life. The Journal of pediatrics. 1998; 132(6):924–33. [PubMed: 9627580]
21. Rinaldo P, Matern D, Bennett MJ. Fatty acid oxidation disorders. Annual review of physiology. 2002; 64:477–502.
22. Badman MK, Pissios P, Kennedy AR, Koukos G, Flier JS, Maratos-Flier E. Hepatic fibroblast growth factor 21 is regulated by PPARalpha and is a key mediator of hepatic lipid metabolism in ketotic states. Cell Metab. 2007; 5(6):426–37. [PubMed: 17550778]
23. Inagaki T, Dutchak P, Zhao G, Ding X, Gautron L, Parameswara V, Li Y, Goetz R, Mohammadi M, Esser V, et al. Endocrine regulation of the fasting response by PPARalpha-mediated induction of fibroblast growth factor 21. Cell Metab. 2007; 5(6):415–25. [PubMed: 17550777]
24. Wheatcroft SB, Kearney MT. IGF-dependent and IGF-independent actions of IGF-binding protein-1 and -2: implications for metabolic homeostasis. Trends Endocrinol Metab. 2009; 20(4): 153–62. [PubMed: 19349193]
25. Hsiao EC, Koniaris LG, Zimmers-Koniaris T, Sebald SM, Huynh TV, Lee SJ. Characterization of growth-differentiation factor 15, a transforming growth factor beta superfamily member induced following liver injury. Molecular and cellular biology. 2000; 20(10):3742–51. [PubMed: 10779363]
26. Johnen H, Lin S, Kuffner T, Brown DA, Tsai VW, Bauskin AR, Wu L, Pankhurst G, Jiang L, Junankar S, et al. Tumor-induced anorexia and weight loss are mediated by the TGF-beta superfamily cytokine MIC-1. Nat Med. 2007; 13(11):1333–40. [PubMed: 17982462]
27. Fisher FM, Maratos-Flier E. Understanding the Physiology of FGF21. Annual review of physiology. 2016; 78:223–41.
28. Fisher FM, Kleiner S, Douris N, Fox EC, Mepani RJ, Verdeguer F, Wu J, Kharitonenkov A, Flier JS, Maratos-Flier E, et al. FGF21 regulates PGC-1alpha and browning of white adipose tissues in adaptive thermogenesis. Genes Dev. 2012; 26(3):271–81. [PubMed: 22302939]
29. Holland WL, Adams AC, Brozinick JT, Bui HH, Miyauchi Y, Kusminski CM, Bauer SM, Wade M, Singhal E, Cheng CC, et al. An FGF21-adiponectin-ceramide axis controls energy expenditure and insulin action in mice. Cell Metab. 2013; 17(5):790–7. [PubMed: 23663742]
30. Lin Z, Tian H, Lam KS, Lin S, Hoo RC, Konishi M, Itoh N, Wang Y, Bornstein SR, Xu A, et al. Adiponectin mediates the metabolic effects of FGF21 on glucose homeostasis and insulin sensitivity in mice. Cell Metab. 2013; 17(5):779–89. [PubMed: 23663741]
31. Wanders RJ, Vreken P, den Boer ME, Wijburg FA, van Gennip AH, LIJ. Disorders of mitochondrial fatty acyl-CoA beta-oxidation. Journal of inherited metabolic disease. 1999; 22(4): 442–87. [PubMed: 10407780]
32. Brivet M, Boutron A, Slama A, Costa C, Thuillier L, Demaugre F, Rabier D, Saudubray JM, Bonnefont JP. Defects in activation and transport of fatty acids. Journal of inherited metabolic disease. 1999; 22(4):428–41. [PubMed: 10407779]
33. Auestad N, Korsak RA, Morrow JW, Edmond J. Fatty acid oxidation and ketogenesis by astrocytes in primary culture. J Neurochem. 1991; 56(4):1376–86. [PubMed: 2002348]
34. Guzman M, Blazquez C. Ketone body synthesis in the brain: possible neuroprotective effects. Prostaglandins, leukotrienes, and essential fatty acids. 2004; 70(3):287–92.
35. Newman JC, Verdin E. Ketone bodies as signaling metabolites. Trends Endocrinol Metab. 2014; 25(1):42–52. [PubMed: 24140022]
36. Kimura I, Inoue D, Maeda T, Hara T, Ichimura A, Miyauchi S, Kobayashi M, Hirasawa A, Tsujimoto G. Short-chain fatty acids and ketones directly regulate sympathetic nervous system via G protein-coupled receptor 41 (GPR41). Proceedings of the National Academy of Sciences of the United States of America. 2011; 108(19):8030–5. [PubMed: 21518883]
37. Taggart AK, Kero J, Gan X, Cai TQ, Cheng K, Ippolito M, Ren N, Kaplan R, Wu K, Wu TJ, et al. (D)-beta-Hydroxybutyrate inhibits adipocyte lipolysis via the nicotinic acid receptor PUMA-G. The Journal of biological chemistry. 2005; 280(29):26649–52. [PubMed: 15929991]

38. Chakravarthy MV, Lodhi IJ, Yin L, Malapaka RR, Xu HE, Turk J, Semenkovich CF. Identification of a physiologically relevant endogenous ligand for PPARalpha in liver. Cell. 2009; 138(3):476–88. [PubMed: 19646743]
39. Chakravarthy MV, Pan Z, Zhu Y, Tordjman K, Schneider JG, Coleman T, Turk J, Semenkovich CF. "New" hepatic fat activates PPARalpha to maintain glucose, lipid, and cholesterol homeostasis. Cell Metab. 2005; 1(5):309–22. [PubMed: 16054078]
40. Chakravarthy MV, Zhu Y, Lopez M, Yin L, Wozniak DF, Coleman T, Hu Z, Wolfgang M, Vidal-Puig A, Lane MD, et al. Brain fatty acid synthase activates PPARalpha to maintain energy homeostasis. J Clin Invest. 2007; 117(9):2539–52. [PubMed: 17694178]
41. Mottillo EP, Bloch AE, Leff T, Granneman JG. Lipolytic products activate peroxisome proliferator-activated receptor (PPAR) alpha and delta in brown adipocytes to match fatty acid oxidation with supply. The Journal of biological chemistry. 2012; 287(30):25038–48. [PubMed: 22685301]
42. Haemmerle G, Moustafa T, Woelkart G, Buttner S, Schmidt A, van de Weijer T, Hesselink M, Jaeger D, Kienesberger PC, Zierler K, et al. ATGL-mediated fat catabolism regulates cardiac mitochondrial function via PPAR-alpha and PGC-1. Nat Med. 2011; 17(9):1076–85. [PubMed: 21857651]
43. Ahmadian M, Abbott MJ, Tang T, Hudak CS, Kim Y, Bruss M, Hellerstein MK, Lee HY, Samuel VT, Shulman GI, et al. Desnutrin/ATGL is regulated by AMPK and is required for a brown adipose phenotype. Cell metabolism. 2011; 13(6):739–48. [PubMed: 21641555]
44. Schoiswohl G, Stefanovic-Racic M, Menke MN, Wills RC, Surlow BA, Basantani MK, Sitnick MT, Cai L, Yazbeck CF, Stolz DB, et al. Impact of reduced ATGL-mediated adipocyte lipolysis on obesity-associated insulin resistance and inflammation in male mice. Endocrinology. 2015; 156(10):3610–24. [PubMed: 26196542]
45. Markan KR, Naber MC, Ameka MK, Anderegg MD, Mangelsdorf DJ, Kliewer SA, Mohammadi M, Potthoff MJ. Circulating FGF21 is liver derived and enhances glucose uptake during refeeding and overfeeding. Diabetes. 2014; 63(12):4057–63. [PubMed: 25008183]
46. Davis RL, Liang C, Edema-Hildebrand F, Riley C, Needham M, Sue CM. Fibroblast growth factor 21 is a sensitive biomarker of mitochondrial disease. Neurology. 2013; 81(21):1819–26. [PubMed: 24142477]
47. Ellis JM, Bowman CE, Wolfgang MJ. Metabolic and Tissue-Specific Regulation of Acyl-CoA Metabolism. PLoS One. 2015; 10(3):e0116587. [PubMed: 25760036]
48. Ellis JM, Wong GW, Wolfgang MJ. Acyl coenzyme A thioesterase 7 regulates neuronal fatty acid metabolism to prevent neurotoxicity. Molecular and cellular biology. 2013; 33(9):1869–82. [PubMed: 23459938]
49. Chace DH, Hillman SL, Van Hove JL, Naylor EW. Rapid diagnosis of MCAD deficiency: quantitative analysis of octanoylcarnitine and other acylcarnitines in newborn blood spots by tandem mass spectrometry. Clinical chemistry. 1997; 43(11):2106–13. [PubMed: 9365395]
50. Sandlers Y, Moser AB, Hubbard WC, Kratz LE, Jones RO, Raymond GV. Combined extraction of acyl carnitines and 26:0 lysophosphatidylcholine from dried blood spots: prospective newborn screening for X-linked adrenoleukodystrophy. Mol Genet Metab. 2012; 105(3):416–20. [PubMed: 22197596]
51. Jiang S, Yan C, Fang QC, Shao ML, Zhang YL, Liu Y, Deng YP, Shan B, Liu JQ, Li HT, et al. Fibroblast growth factor 21 is regulated by the IRE1alpha-XBP1 branch of the unfolded protein response and counteracts endoplasmic reticulum stress-induced hepatic steatosis. The Journal of biological chemistry. 2014; 289(43):29751–65. [PubMed: 25170079]

Highlights

- Hepatic fatty acid oxidation (FAO) is critical for liver physiology during starvation.
- Hepatic FAO suppresses adipose lipolysis and systemic catabolism.
- Upon fasting, loss of hepatic FAO induces Pparα target genes in the liver.
- A ketogenic diet induces severe lipolysis and lethality in hepatic FAO deficient mice.

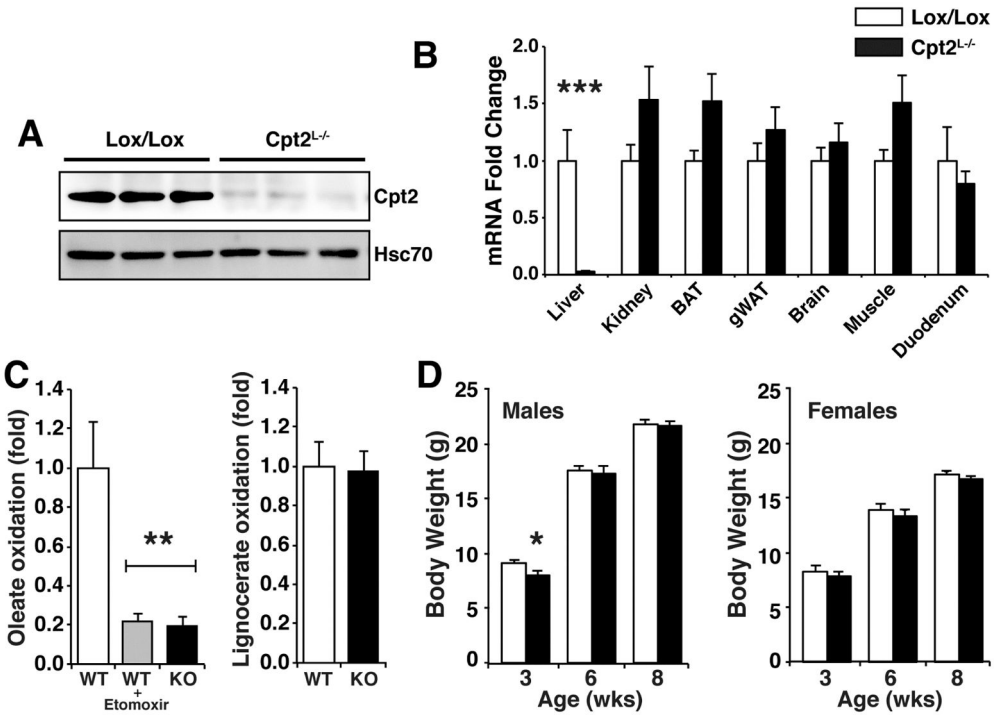

Figure 1. Characterization of mice with a liver specific KO of CPT2

(A) Western blot for CPT2 in liver of $Cpt2^{lox/lox}$ and $Cpt2^{L-/-}$ mice.

(B) mRNA for *Cpt2* across different tissues (n=6).

(C) Oxidation of 1-^{14}C-oleic acid and 1-^{14}C-Lignoceric acid to $^{14}CO_2$ in liver slices of $Cpt2^{lox/lox}$ and $Cpt2^{L-/-}$ mice (n=5).

(D) Body weights of $Cpt2^{lox/lox}$ and $Cpt2^{L-/-}$ male and female mice fed a normal chow diet (males, n=14-23; females, n=8-12).

Data are expressed as mean ± SEM. *p<0.05; **p<0.01; ***p<0.001.

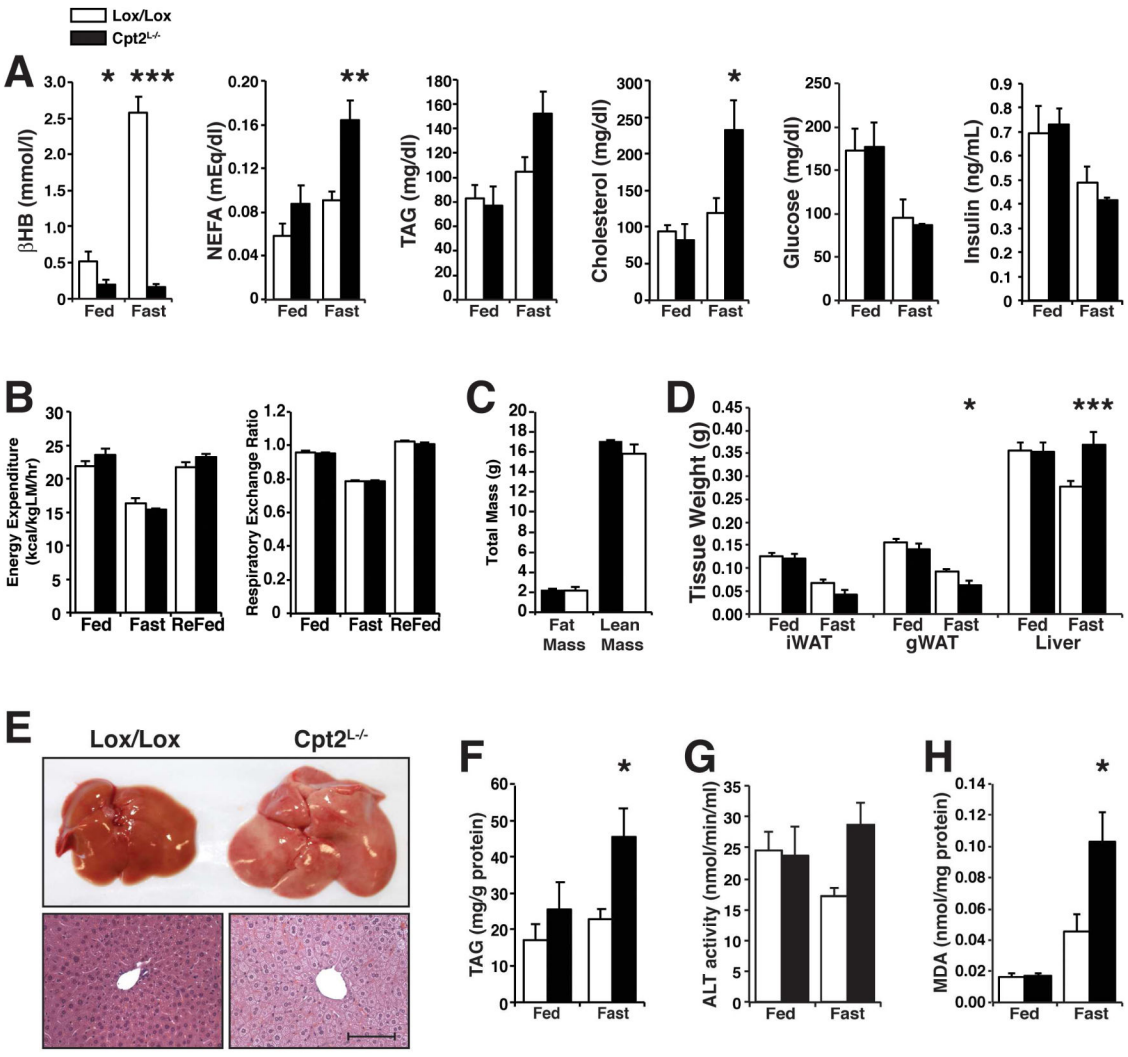

Figure 2. Liver and systemic deficits in fed and 24hr fasted Cpt2$^{L-/-}$ mice

(A) Serum metabolites in Cpt2$^{lox/lox}$ and Cpt2$^{L-/-}$ mice (n=6).

(B) Energy expenditure and respiratory exchange ratio of Cpt2$^{lox/lox}$ and Cpt2$^{L-/-}$ mice under fed, fast and refed conditions (males, n=5-7).

(C) Total fat and lean mass of Cpt2$^{lox/lox}$ and Cpt2$^{L-/-}$ male mice (n=5-7).

(D) Wet weights of fed or 24 hour fasted iWAT, gWAT, and liver for Cpt2$^{lox/lox}$ and Cpt2$^{L-/-}$ mice (n=6-10).

(E) Gross and histological morphology of livers from 24 hr fasted Cpt2$^{lox/lox}$ and Cpt2$^{L-/-}$ mice. Scale bar equals 100 μM.

(F) Triglyceride levels from liver homogenates of fed and 24 hr fasted Cpt2$^{lox/lox}$ and Cpt2$^{L-/-}$ mice (n=5).

(G) Liver damage measured by serum ALT activity of fed and 24h fasted Cpt2$^{lox/lox}$ and Cpt2$^{L-/-}$ mice (n=5).

(H) TBARS assay measuring lipid peroxidation from liver of fed and 24 hr fasted Cpt2$^{lox/lox}$ and Cpt2$^{L-/-}$ mice (n=5).

Data are expressed as mean ± SEM. *p<0.05; **p<0.01; ***p<0.001.

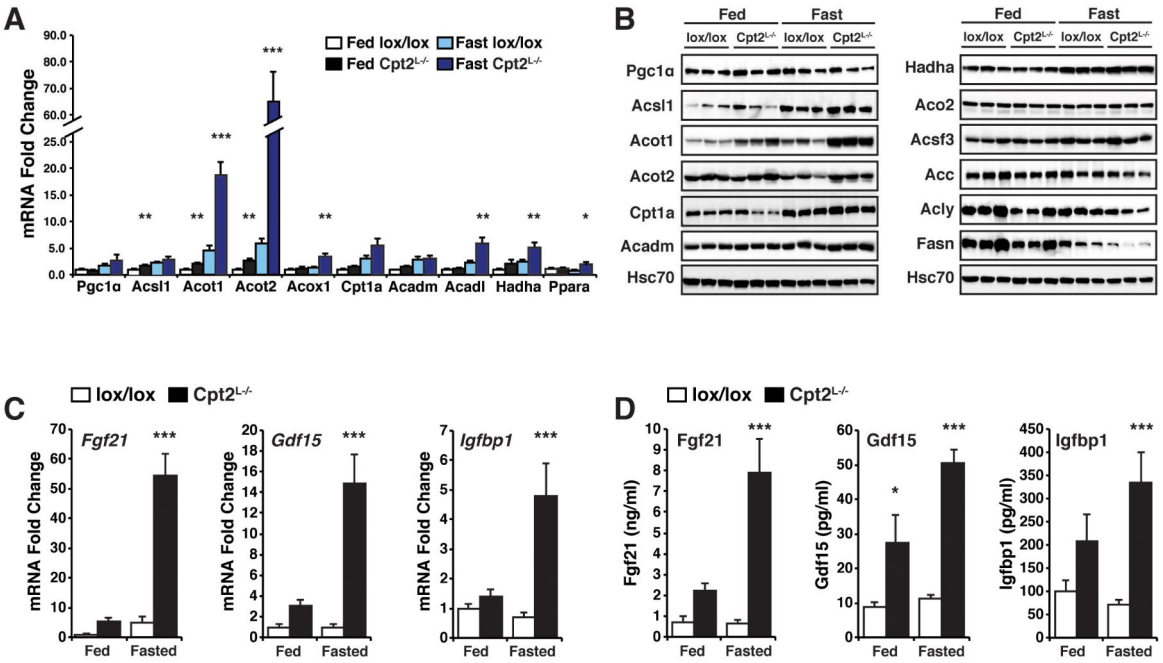

Figure 3. Loss of hepatic fatty acid oxidation induces expression of fatty acid oxidative genes

(A) Gene expression of fatty acid oxidation genes in liver of fed and 24 hr fasted $Cpt2^{lox/lox}$ and $Cpt2^{L-/-}$ mice (n=6).

(B) Western blots of proteins in fatty acid metabolism. Composite of 8 blots. All blots were normalized to Hsc70 (Figure S2).

(C) Liver mRNA (n=6) of Fgf21, Gdf15 and Igfbp1 in fed and 24 hr fasted $Cpt2^{lox/lox}$ and $Cpt2^{L-/-}$ mice.

(D) Serum concentrations (n=8) of Fgf21, Gdf15 and Igfbp1 in fed and 24 hr fasted $Cpt2^{lox/lox}$ and $Cpt2^{L-/-}$ mice.

Data are expressed as mean ± SEM. *p<0.05; **p<0.01; ***p<0.001.

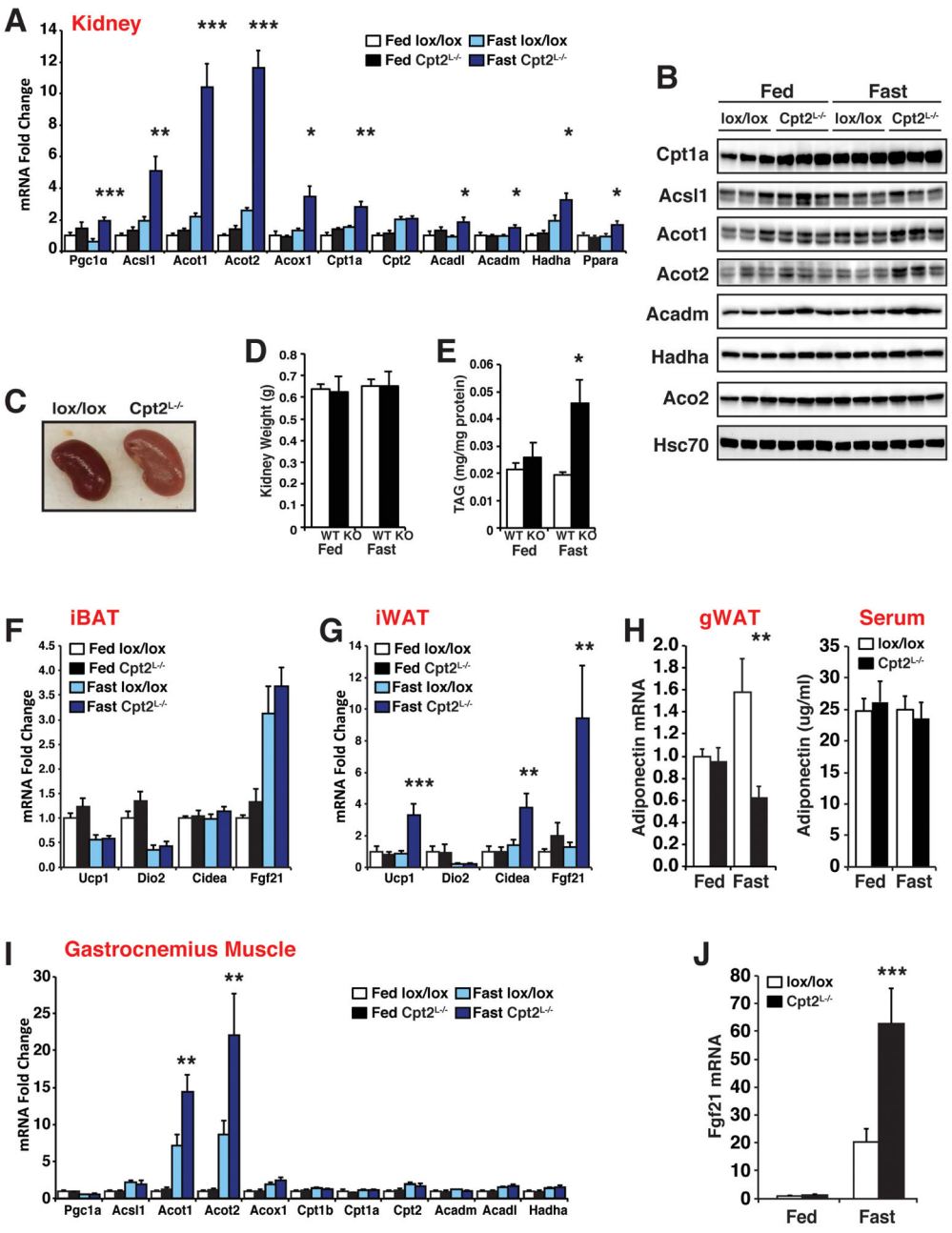

Figure 4. Loss of hepatic fatty acid oxidation results in compensation from the kidney, muscle and adipose tissue

(A) Gene expression of fatty acid oxidation genes in the kidney of fed and 24 hr fasted $Cpt2^{lox/lox}$ and $Cpt2^{L-/-}$ mice (n=6).

(B) Western blots of proteins in fatty acid metabolism. Composite of 5 blots. All blots were normalized to Hsc70 (Figure S3).

(C) Gross kidney morphology in 24 hr fasted $Cpt2^{lox/lox}$ and $Cpt2^{L-/-}$ mice.

(D) Kidney wet weight of fed and 24 hr fasted $Cpt2^{lox/lox}$ and $Cpt2^{L-/-}$ mice (n=6-10).

(E) Kidney TAG content of fed and 24 hr fasted $Cpt2^{lox/lox}$ and $Cpt2^{L-/-}$ mice (n=5).

(F) iBAT gene expression of fed and 24 hr fasted $Cpt2^{lox/lox}$ and $Cpt2^{L-/-}$ mice (n=6).

(G) iWAT gene expression of fed and 24 hr fasted $Cpt2^{lox/lox}$ and $Cpt2^{L-/-}$ mice (n=6).
(H) gWAT adiponectin mRNA (n=6) and Adiponectin serum concentration (n=8) of fed and 24 hr fasted $Cpt2^{lox/lox}$ and $Cpt2^{L-/-}$ mice.
(I) Gene expression of fatty acid oxidation genes in the gastrocnemius muscle of fed and 24 hr fasted $Cpt2^{lox/lox}$ and $Cpt2^{L-/-}$ mice (n=6).
(J) Gastrocnemius muscle mRNA of *Fgf21* in fed and 24 hr fasted $Cpt2^{lox/lox}$ and $Cpt2^{L-/-}$ mice (n=6).
Data are expressed as mean ± SEM. *p<0.05; **p<0.01; ***p<0.001.

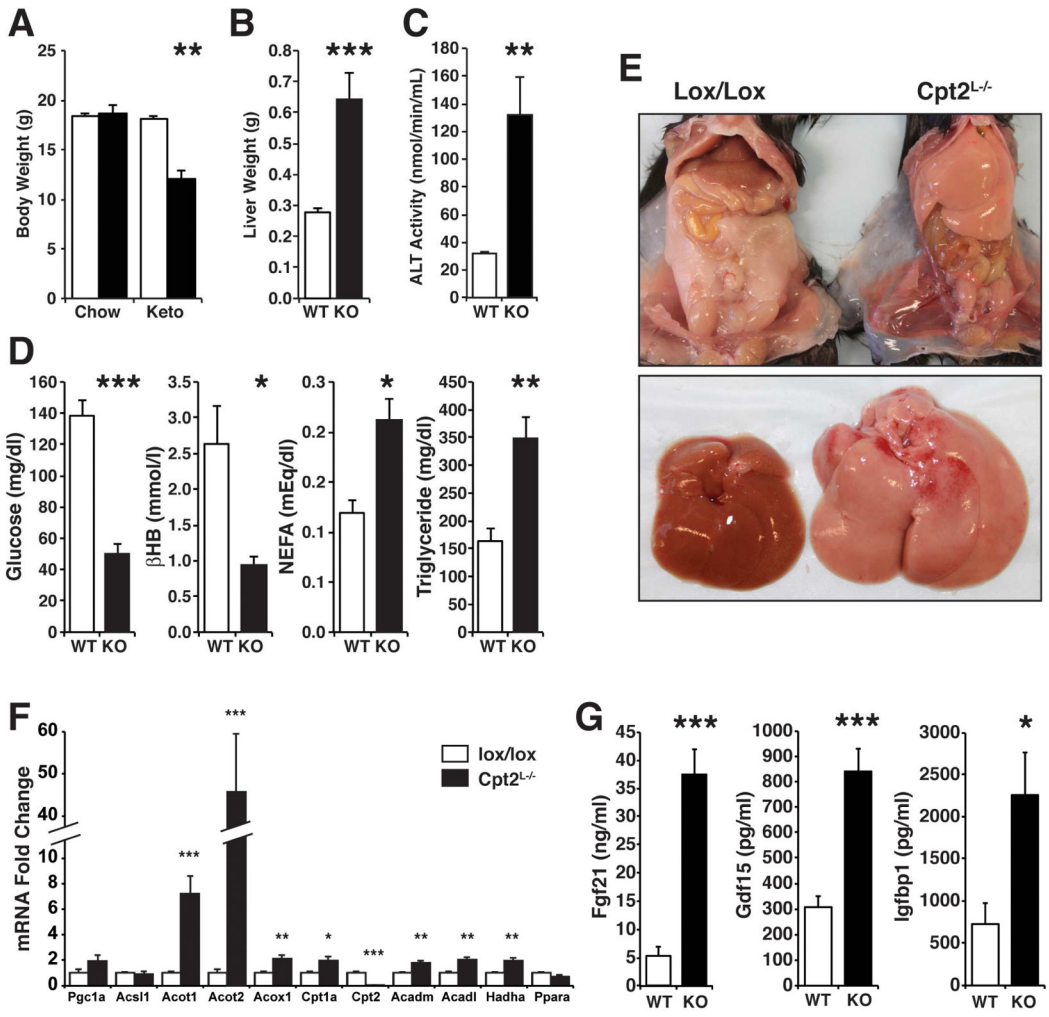

Figure 5. A ketogenic diet results in hypoglycemia, a depletion of adipose triglyceride and eventually lethality in Cpt2$^{L-/-}$ mice

(A) Body weights of Cpt2$^{lox/lox}$ and Cpt2$^{L-/-}$ mice fed a normal chow or ketogenic diet for 6 days (normal chow, n=6-10; ketogenic diet, n=5-6).

(B) Wet weight of liver from Cpt2$^{lox/lox}$ and Cpt2$^{L-/-}$ mice fed a ketogenic diet for 6 days (n=5-6).

(C) Liver damage measured by serum ALT activity of Cpt2$^{lox/lox}$ and Cpt2$^{L-/-}$ mice fed a ketogenic diet (n=5).

(D) Serum metabolites in Cpt2$^{lox/lox}$ and Cpt2$^{L-/-}$ mice after a 6-day ketogenic diet (n=5-6).

(E) Gross morphology of Cpt2$^{lox/lox}$ and Cpt2$^{L-/-}$ mice fed a ketogenic diet.

(F) Gene expression of fatty acid oxidation genes in the liver of Cpt2$^{lox/lox}$ and Cpt2$^{L-/-}$ mice fed a ketogenic diet (n=6).

(G) Serum concentrations of Fgf21, Gdf15 and Igfbp1 of Cpt2$^{lox/lox}$ and Cpt2$^{L-/-}$ mice fed a ketogenic diet (n=6).

Data are expressed as mean ± SEM. *p<0.05; **p<0.01; ***p<0.001.

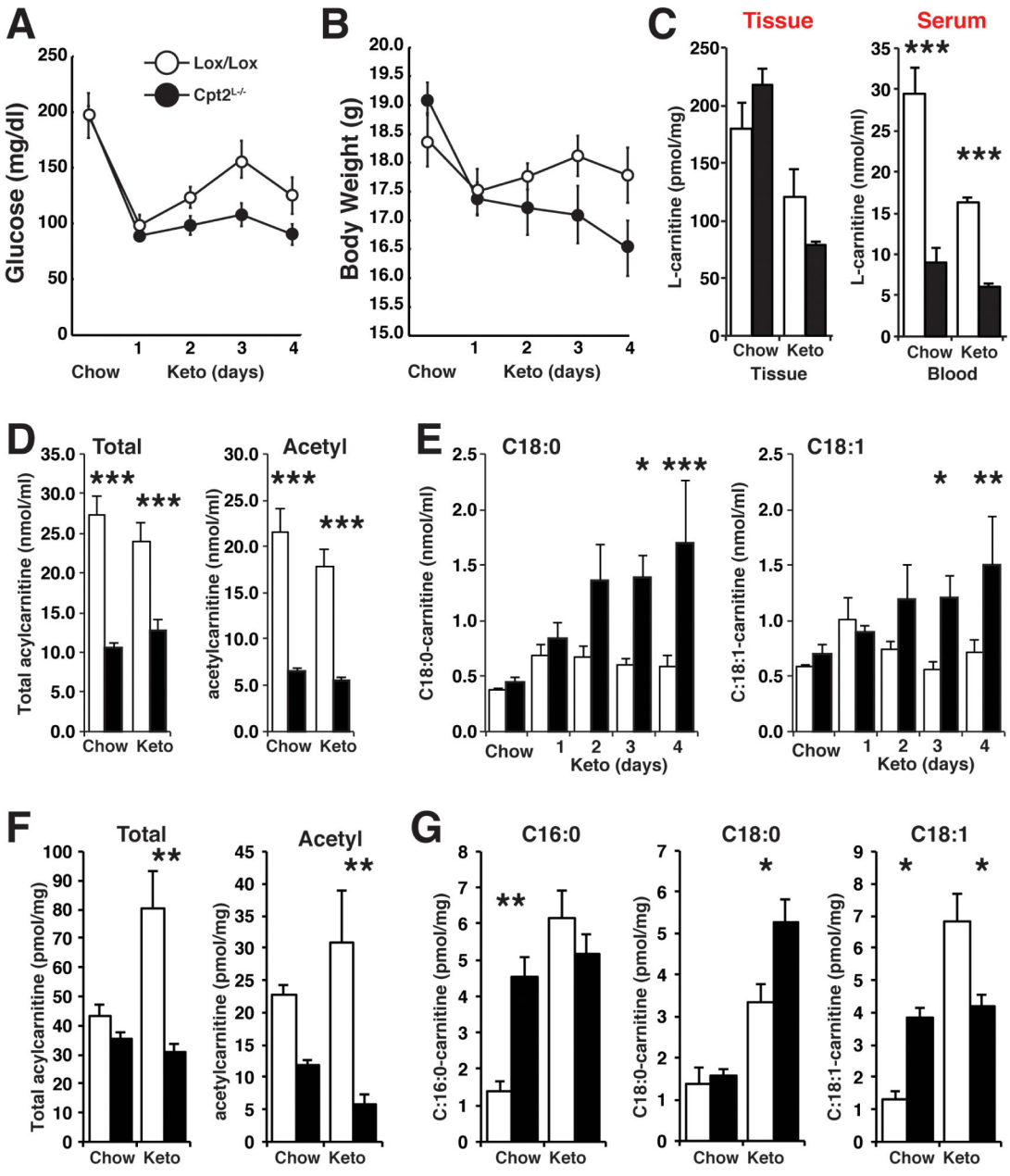

Figure 6. Time course of body weight, blood glucose and acylcarnitines in Cpt2$^{L-/-}$ mice fed a ketogenic diet

(A) Blood glucose of Cpt2$^{lox/lox}$ and Cpt2$^{L-/-}$ mice during a 4-day ketogenic diet (n=5).

(B) Body weight of Cpt2$^{lox/lox}$ and Cpt2$^{L-/-}$ mice during a 4-day ketogenic diet (n=5).

(C) Liver and blood L-carnitine of Cpt2$^{lox/lox}$ and Cpt2$^{L-/-}$ mice following a 4-day ketogenic diet (n=5).

(D) Total blood acylcarnitines and acetylcarnitine of Cpt2$^{lox/lox}$ and Cpt2$^{L-/-}$ mice following a 4-day ketogenic diet (n=5).

(E) Daily blood long chain (C18:0, C18:1) acylcarnitines of Cpt2$^{lox/lox}$ and Cpt2$^{L-/-}$ mice during a 4-day ketogenic diet (n=5).

(F) Total liver acylcarnitines and acetylcarnitine of $Cpt2^{lox/lox}$ and $Cpt2^{L-/-}$ mice following a 4-day ketogenic diet (n=4-5).
(G) Total liver long chain (C16:0, C18:0, C18:1) acylcarnitines and acetylcarnitine of $Cpt2^{lox/lox}$ and $Cpt2^{L-/-}$ mice following a 4-day ketogenic diet (n=4-5).
Data are expressed as mean ± SEM. *p<0.05; **p<0.01; ***p<0.001.

Table 1

Fasting and diet induced gene expression in $Cpt2^{L-/-}$ liver.

	Fasted	Fed		Fasted		Ketogenic Diet	
Gene	**Array KO/WT**	**Lox/Lox**	**Cpt2L−/−**	**Lox/Lox**	**Cpt2L−/−**	**Lox/Lox**	**Cpt2L−/−**
Pdk4	30.5	1.0 ± 0.17	3.9 ± 0.39	1.2 ± 0.30	99.0 ± 16.22***	1.0 ± 0.34	178.9 ± 41.42 **
Elovl7	13.3	1.0 ± 0.17	2.1 ± 0.33	0.9 ± 0.24	174.9 ± 31.58***	1.0 ± 0.46	58.7 ± 9.38***
Gpnmb	10.2	1.0 ± 0.26	2.2 ± 0.27	2.1 ± 0.51	301.7 ± 67.18***	1.0 ± 0.35	134.9 ± 12.60***
Cpt1b	8.9	1.0 ± 0.10	4.4 ± 1.25	6.1 ± 2.42	84.5 ± 14.39***	1.0 ± 0.23	9.9 ± 2.95 *
Phospho1	7.6	1.0 ± 0.20	3.5 ± 0.22	1.8 ± 0.50	30.2 ± 7.71***	1.0 ± 0.26	15.3 ± 3.18***
Fgf21	6.0	1.0 ± 0.15	5.4 ± 1.00	4.9 ± 2.12	54.6 ± 7.02***	1.0 ± 0.26	13.9 ± 3.18 **
Fabp3	5.8	1.0 ± 0.18	1.4 ± 0.24	2.4 ± 0.31	161.1 ± 21.31***	1.0 ± 0.19	32.0 ± 3.71***
Atf3	5.4	1.0 ± 0.16	2.1 ± 0.43	0.9 ± 0.10	28.4 ± 4.18***	1.0 ± 0.40	15.8 ± 2.58***
Cd68	5.0	1.0 ± 0.11	1.2 ± 0.27	0.8 ± 0.18	8.0 ± 1.09***	1.0 ± 0.19	2.1 ± 0.15 **
Igfbp1	4.4	1.0 ± 0.16	1.4 ± 0.25	0.7 ± 0.18	4.8 ± 1.08***	1.0 ± 0.33	42.6 ± 13.62 *
Acot2	4.4	1.0 ± 0.23	2.6 ± 0.52	5.8 ± 0.96	65.2 ± 11.33***	1.0 ± 0.30	45.7 ± 13.80***
Plin4	4.2	1.0 ± 0.17	1.0 ± 0.25	1.0 ± 0.23	7.6 ± 1.04***	1.0 ± 0.12	6.5 ± 1.07***
Jun	3.1	1.0 ± 0.17	1.8 ± 0.40	1.3 ± 0.42	5.8 ± 1.42***	1.0 ± 0.22	4.4 ± 0.46***
Cd36	3.0	1.0 ± 0.15	1.7 ± 0.25	1.5 ± 0.28	9.9 ± 2.51***	1.0 ± 0.26	7.5 ± 0.94***
Gdf15	3.0	1.0 ± 0.24	3.1 ± 0.49	1.0 ± 0.24	14.9 ± 2.81***	1.0 ± 0.33	10.1 ± 1.47***
Acot1	3.0	1.0 ± 0.10	2.1 ± 0.23	4.5 ± 1.05	18.7 ± 2.47***	1.0 ± 0.12	7.2 ± 1.41***
Agpat9	2.9	1.0 ± 0.15	4.0 ± 0.84	2.7 ± 0.49	10.1 ± 1.80***	1.0 ± 0.21	3.2 ± 0.52 **
Pex11a	2.9	1.0 ± 0.08	1.8 ± 0.30	1.4 ± 0.35	4.5 ± 0.73***	1.0 ± 0.07	2.2 ± 0.24***
Ehhadh	2.5	1.0 ± 0.21	1.4 ± 0.27	8.7 ± 1.54	49.4 ± 6.72***	1.0 ± 0.16	10.1 ± 1.95***
Acot6	2.5	1.0 ± 0.22	2.3 ± 0.44	2.2 ± 0.52	6.9 ± 1.59***	1.0 ± 0.20	1.8 ± 0.43
Myc	2.4	1.0 ± 0.17	1.2 ± 0.12	3.8 ± 0.95	10.8 ± 2.23***	1.0 ± 0.28	5.4 ± 1.24 **
Gpd2	2.2	1.0 ± 0.16	1.3 ± 0.29	0.7 ± 0.12	1.9 ± 0.38**	1.0 ± 0.20	2.7 ± 0.59 **
Mtor	2.2	1.0 ± 0.17	1.6 ± 0.28	1.3 ± 0.14	3.2 ± 0.51***	1.0 ± 0.07	2.0 ± 0.43 *

	Fasted	Fed		Fasted		Ketogenic Diet	
Gene	**Array KO/WT**	**Lox/Lox**	**Cpt2L−/−**	**Lox/Lox**	**Cpt2L−/−**	**Lox/Lox**	**Cpt2L−/−**
Plin5	2.2	1.0 ± 0.15	1.1 ± 0.28	1.6 ± 0.32	5.6 ± 0.55***	1.0 ± 0.19	4.4 ± 1.14 **
Plin3	2.2	1.0 ± 0.13	1.3 ± 0.19	1.2 ± 0.18	3.5 ± 0.46***	1.0 ± 0.15	2.8 ± 0.30***

Microarray on liver of 24 hr fasted $Cpt2^{lox/lox}$ and $Cpt2^{L-/-}$ mice (n=3). Validation by qRTPCR in liver of fed and 24 hr fasted $Cpt2^{lox/lox}$ and $Cpt2^{L-/-}$ mice (n=6). qRTPCR in liver of 6 day ketogenic diet fed $Cpt2^{lox/lox}$ and $Cpt2^{L-/-}$ mice (n=6). Data are expressed as mean ± SEM.

*p<0.05;

**p<0.01;

***p<0.001.